Stiffness of a Fracture from AVO Inversion Incorporating Linear Slip Boundary Condition - Experimental Investigation

Minato, Shohei; Ghose, Ranajit; Osukuku, G.

Important note
To cite this publication, please use the final published version (if applicable).
Please check the document version above.

Stiffness of a fracture from AVO inversion incorporating linear slip boundary condition: experimental investigation

Shohei Minato[1], Ranajit Ghose[1], Godfred Osukuku[1]

[1]*Delft University of Technology, Section of Applied Geophysics and Petrophysics, Department of Geoscience and Engineering, Delft, The Netherlands. E-mail: s.minato-1@tudelft.nl;
r.ghose@tudelft.nl;*

SUMMARY

Characterizing fracture is important in order to understand how groundwater is transported and stored in fractured environments, to assess contaminant transport through fractures, as well to evaluate the mechanical behaviour of a fractured rock mass. In this research, we have investigated through careful laboratory experiments the amplitude versus offset (AVO) response of seismic reflections from a fracture. We use the linear slip boundary condition at the fracture and estimate the angle-dependent reflection response due to a single fracture. The observed angle-dependent reflectivity is inverted to obtain the fracture compliance and aperture. Two detailed laboratory experiments are performed - one using laterally homogeneous fracture and another using laterally heterogeneous fracture (partly air-filled and partly water-filled). Our results demonstrate that normal compliance (inverse stiffness) of a fracture can be quite accurately estimated from the AVO inversion of P-P reflected waves. It is also possible to obtain the non-zero tangential compliance. The existence of fluid in the fracture can be predicted. Distinction of the fracture infills and quantification of the fracture aperture are possible. This finding will be crucial for numerous new applications in civil and geotechnical engineering, hydrogeophysics, as well as in other areas of earth sciences and non-destructive material testing.

Introduction

Understanding how groundwater is transported and stored in fractured environments using traditional hydrologic measurements presents a unique challenge because groundwater is channelled into narrow zones that are difficult to detect and characterize. Characterizing fractures is, therefore, important for understanding the permeable zone, preferential flow paths and fluid migration pattern, modelling fluid flow and contaminant transport in fractured rocks, and assessing the vulnerability of the groundwater to mine drainage problems. The significance of distinguishing and mapping water-filled and dry fractured zones is high. Further, in a brittle rock mass the presence of a fracture network results in the rock mass being deformable, weaker, and more permeable. This has major implications in civil and geotechnical engineering. In this case, the stiffness of the fracture, which is a function of fracture aperture, roughness and fracture infill, is a key determinant.

Non-invasive geophysical methods provide a way to image the subsurface over large spatial scales, providing the necessary insight to guide more traditional hydrological and geotechnical investigations in fractured systems. Various geophysical methods have so far been used to map and characterize fractures. In this regard, seismic methods have a unique relevance when the goal is to evaluate the mechanical properties/stiffness of the fractured medium or individual fractures of intermediate to large scale. In general, seismic characterization has so far utilized the changes in the effective acoustic/elastic properties over a certain volume, that occur due to the presence of aligned fractures. With the availability of higher frequencies and improved surface and downhole acquisition systems, lately it has been possible to record reflected seismic waves from subsurface fractures. Observing such reflections depends particularly on the seismic wavelength relative to the scale of the fracture.

In this research, we have investigated the amplitude versus offset (AVO) response of seismic reflections from a fracture. We use the linear slip boundary condition at the fracture and estimate the angle-dependent reflection response due to a single fracture. This is used to invert the observed angle-dependent reflectivity to estimate fracture compliance (inverse of stiffness) and aperture. Two detailed laboratory experiments are performed - one using laterally homogeneous fracture and another using laterally heterogeneous fracture (partly air-filled and partly water-filled). The results of AVO inversion of the experimental data using the theoretical expressions for the AVO response of a nonwelded (linear slip) boundary show encouraging possibilities.

AVO response of a fracture: theoretical basis

Though well-known for layer boundaries (i.e., welded interfaces), the AVO response of a nonwelded interface has not been utilized so far to estimate the fracture compliance. This is mainly because of the lack of high frequencies in the conventional seismic field data. However, as mentioned above, the situation has changed in the recent years, thus motivating us to look into the AVO response of fractures, which are nonwelded interfaces (Nagy, 1992). As opposed to a welded boundary (layer interface) across which both elastic stress (or traction) and displacements are continuous, a nonwelded interface is an interface across which stress is continuous but elastic displacement is discontinuous (e.g., Schoenberg, 1980). This boundary condition can be written as $\Delta u = Zt$, where Δu and t are, respectively, the jump in elastic displacement vector and the traction vector in the fracture-oriented Cartesian coordinate. Assuming a rotationally invariant compliance matrix (Schoenberg, 1980), the fracture compliance matrix Z consists of η_N and η_T (normal and tangential compliances, respectively) as $Z=\text{diag}(\eta_T, \eta_T, \eta_N)$.

The explicit form of P- and SV-wave reflection coefficients due to an incident P-wave on a nonwelded interface located within a homogeneous medium was derived earlier (Chaisri and Krebes, 2000):

$$R_{PP} = [\omega^2 \eta_N \eta_T KL + 2i\omega\rho\eta(\eta_N\gamma^2 - \eta_T\chi^2\xi^2)]D^{-1}, \tag{1}$$

$$R_{PS} = -2\gamma\chi\xi\frac{V_P}{V_S}\left[\omega^2\eta_N\eta_T K + i\omega\rho(\eta_T\xi + \eta_N\eta)\right]D^{-1}, \tag{2}$$

where,

$$D = (2\rho\xi - i\omega\eta_N K)(2\rho\eta - i\omega\eta_T K), \tag{3}$$

$$\chi = 2\rho V_S^2 p, \tag{4}$$

$$\gamma = \rho(1 - 2V_s^2 p^2), \tag{5}$$

$$\xi = \frac{\cos\theta_{PP}}{V_P}, \tag{6}$$

$$\eta = \frac{\cos\theta_{PS}}{V_S}, \tag{7}$$

$$K = \gamma^2 + \chi^2\xi\eta, \tag{8}$$

and $L = \gamma^2 - \chi^2\xi\eta$. $\tag{9}$

Here p is the ray parameter ($p = \sin\theta_{PP}/V_P$) and θ_{PS} is the angle of the reflected S wave.

Laboratory experiments and results

We consider a fracture as a thin, parallel-wall layer filled with a soft material, which is often used to represent hydraulic fractures. In this case the fracture compliance can be represented as (e.g., Baik and Thomson, 1984; Liu et al., 2000):

$$\eta_N = \frac{d}{\lambda' + 2\mu'}, \tag{10}$$

$$\eta_T = \frac{d}{\mu'}, \tag{11}$$

where μ' and λ' are Lame constants of the fracture infill, and d is the fracture aperture. Note that the nonwelded interface representation and the application of the AVO inversion that we will discuss in this study are not limited to only a thin, parallel-wall layer model.

Experiment 1: Our experimental setup consists of two aluminium blocks with parallel and smooth surfaces (Figure 1). We assume that the aluminium block is homogeneous and isotropic (V_P=6380 m/s, V_S= 3150 m/s and ρ=2700 kg/m^3). An artificial horizontal fracture is simulated by installing spacers of known thickness (100 μm) between the two blocks. In the first experiment, we install seven longitudinal transducers (Panametrics V103) for an array-seismic measurement (one transmitter and six receiver). The interval between the transducers is 3.5 cm; thus resulting in 6 different incidence angles in the range 5.8˚-31.4˚ for P-P reflections and 7.8˚-41.2˚ for P-S reflections. We generate source signals (truncated sinusoid) with 0.7 MHz center frequency.

We observe the P-P reflections for the dry and the wet fractures at the receiver array (six incidence angles) after bandpass (0.01-1.8 MHz) filtering and muting around the P-P-reflections (Figure 2a). We assume that the difference between the dry and the wet fracture response is only in the reflection coefficients at the fracture and that the incident wave at the fracture and the effect of propagation (e.g., geometrical spreading and attenuation in aluminium) are identical between dry and wet conditions. Because the dry fracture responses are equivalent to the free-surface ones, we calculate the angle- and frequency-dependent P-P reflection coefficient of the wet fracture as follows:

$$R_{PP}^{Wet}(\omega,\theta_{PP}) = R_{PP}^{FS}(\theta_{PP})\frac{D^{Wet}(\omega,\theta_{PP})}{D^{Dry}(\omega,\theta_{PP})}, \tag{12}$$

where R^{FS} denotes the free-surface reflection coefficient (e.g., Aki and Richards, 2002). D^{Wet} and D^{Dry} are the P-P reflection responses of the wet and dry fracture, respectively.

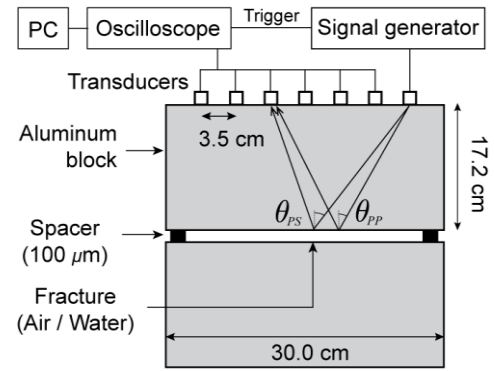The reflection coefficient of the wet fracture is estimated using
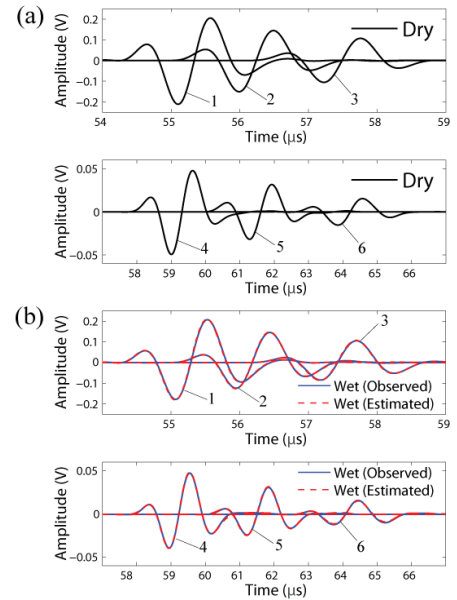

Figure 1: Experimental setup

Figure 2: Observed angle-dependent P-P reflection responses (solid line) for (a) dry and (b) water-filled fractures. The dashed line shows the estimated wet fracture response using the observed dry fracture response. The numbers 1 to 6 represent 6 different incidence angles.

a least-square fitting of the observed coefficients with the theoretical coefficients for a nonwelded interface. The estimated reflection coefficient clearly demonstrates the AVO effect for the nonwelded interface (Figure 3a). The estimated values of η_N at different incidence angles are summarized in Figure 3b. Finally, the predicted waveforms of the wet fracture obtained using the estimated values of η_N match quite well with the observed angle-dependent reflection responses (red lines in Figure 2b). Using the value of the bulk modulus of water (2.2 GPa), we estimated the effective aperture of the fluid-filled fracture from η_N, using equation 10. When we compare the estimated values of the fracture aperture with the true aperture value, we find that the nonwelded interface model estimates reasonably well the fracture aperture for all incidence angles.

Experiment 2: In this experiment, we acquire the reflection seismic dataset in the laboratory in common midpoint shooting mode. The condition of the fracture surface, i.e., wet (water filled) or dry (air-filled), is affected by lifting the top
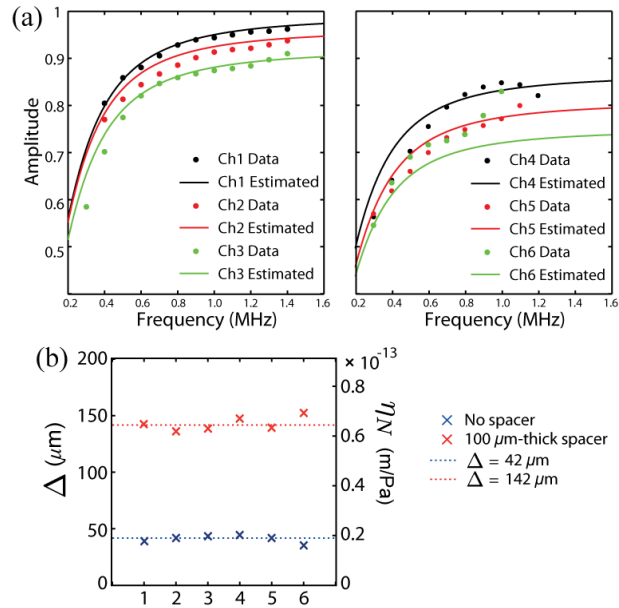

Figure 3: (a) Observed (dots) and estimated (solid line) P-P reflection coefficients of wet fracture using least square inversion. (b) Estimated normal compliances and aperture of the fracture estimated for 6 different incidence angles. Red dotted line shows the true aperture.

aluminium block, applying/cleaning fluid at the fracture surface, and carefully lowering the top block to the original position. The transducer coupling remains constant throughout the experiments. A fixed source-receiver array is moved laterally using a moving template (Figure 4a). This results in a CMP fold distribution as shown in Figure 4b. We further introduce a heterogeneity in fluid distribution along the fracture: we create a wet region and an adjacent dry region in the fracture. The transducers and the center frequency of the source signal are same as in the previous experiment. The reproducibility of the tests is ensured. Note that, for AVO inversion, obviously only the specular reflections are used; however, the full scattered wavefield has also been recently used to predict the lateral heterogeneity in fracture compliance (Minato and Ghose, 2013; 2014; 2016).
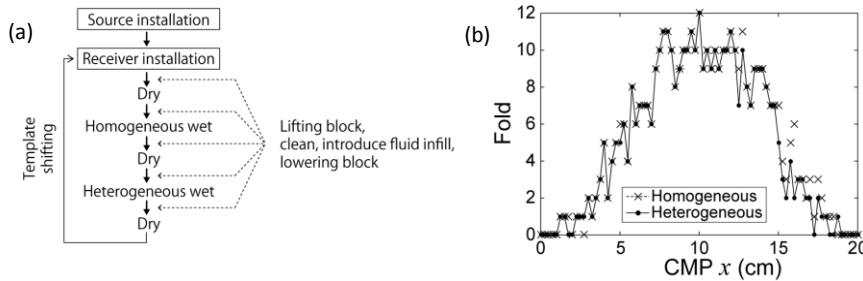

Figure 4: (a) CMP data acquisition in lab: experimental procedure, (b) CMP fold distribution

After data acquisition, data are sorted to create CMP gathers. CMP spacing is 0.25 cm. AVO inversion is next performed through minimizing the following misfit function:

$$S(\eta_N) = \frac{\sqrt{\sum_i \sum_j (|R_{PP}^{obs}(\omega_i, \theta_j)| - |R_{PP}^{est}(\omega_i, \theta_j, \eta_N)|)^2}}{\sqrt{\sum_i \sum_j |R_{PP}^{obs}(\omega_i, \theta_j)|^2}} \,, \tag{13}$$

where ω is frequency, θ is incidence angle, i and j represent the respective components.

Figure 5 shows the misfit function to estimate η_N of the fracture. Figure 6 shows the estimated values of η_N at each CMP for the homogeneously wet fracture (crosses) and the heterogeneously wet fracture (filled circle). Note that the values of η_N at the wet region of the heterogeneously wet fracture very well correspond to those of the homogeneously wet fracture. The transition from dry to wet fracture is reasonably well estimated. Considering the known fracture aperture and the presence of air bubble in the water infill, the effective bulk

modulus of the fracture infill is calculated using mixing rule for bulk modulus (Reuss average) and the estimated η_N (equation 10). We find that our estimated η_N can be explained by very realistic amount of the air bubbles present in water.

Conclusion

Our results demonstrate that normal compliance (inverse stiffness) of a fracture can be quite accurately estimated from AVO inversion of P-P reflected waves. It is also possible to obtain the non-zero tangential compliance. Although, not illustrated in this abstract, we find that supplementing converted P-S reflection information greatly improves the tangential compliance estimates. The existence of fluid in the fracture can be predicted. Distinction of the fracture infill and quantification of the fracture aperture are possible. This finding will be crucial for numerous new applications in civil and geotechnical engineering, hydrogeophysics, as well as in other areas of earth sciences and non-destructive material testing.
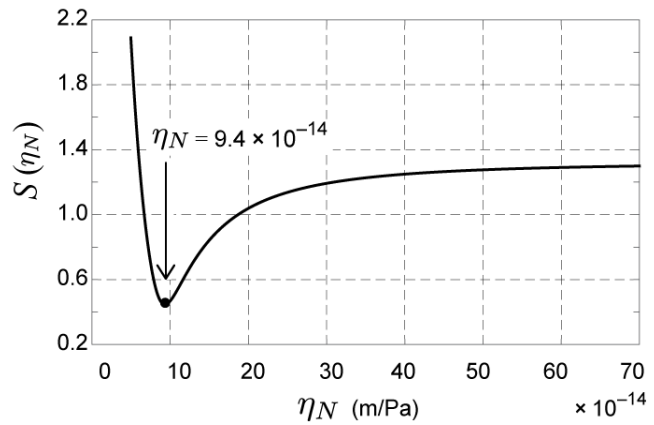
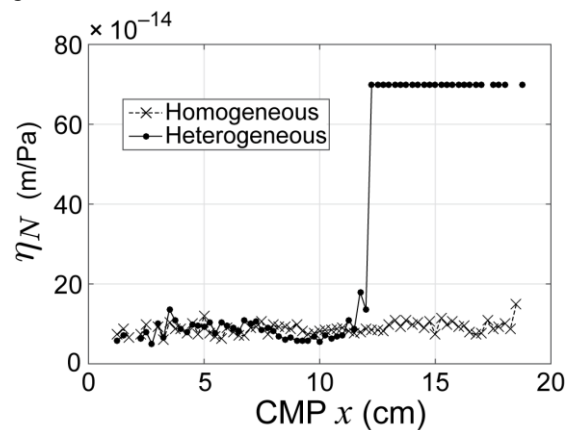Figure 5: The misfit function to estimate the normal compliance from The observed AVO response.

Figure 6: The estimated values of the normal compliance at each CMP for the homogeneously wet and heterogeneously wet fractures.

References
Aki, K. and Richards, R. B. [2002] Quantitative Seismology, 2nd edition, University Science Books.
Baik, J. and Thompson, R. B. [1984] Ultrasonic scattering from imperfect interfaces: a quasi-static model, Journal of Nondestructive Evaluation, 4, 177-196.
Chaisri, S. and Krebes, E. S. [2000] Exact and approximate formulas for P-SV reflection and transmission coefficients for a nonwelded contact interface: J. Geophysical Research: Solid Earth, 105, 28045-28054.
Liu, E., Hudson, J., and Pointer, T. [2000] Equivalent medium representation of fractured rock, Journal of Geophysical Research, 105, 2981-3000.
Minato, S. and Ghose, R. [2013] Inverse scattering solution for the spatially heterogeneous compliance of a single fracture, Geophysical Journal International, 195, 1878-1891.
Minato, S. and Ghose, R. [2014] Imaging and characterization of a subhorizontal non-welded interface from point source elastic response, Geophysical Journal International, 197, 1090-1095.
Minato, S. and Ghose, R. [2016] Enhanced characterization of fracture compliance heterogeneity using multiple reflections and data-driven Green's function retrieval, Journal of Geophysical Research: Solid Earth, 121, 2813-2836.
Nagy, P. [1992] Ultrasonic classification of imperfect interfaces, J. Nondestructive Evaluation, 11, 127-139.
Schoenberg, M. [1980] Elastic wave behaviour across linear slip interfaces, JASA, 68, 1516-1521.